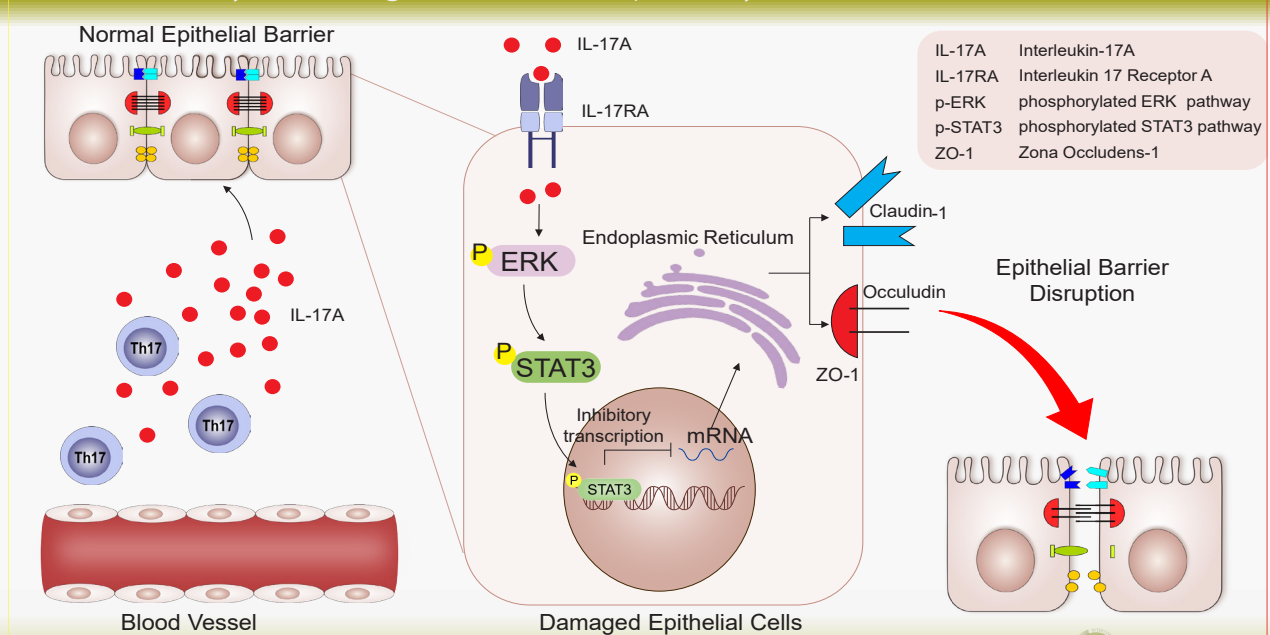


# IL-17A disrupts the nasal mucosal epithelial barrier in patients with chronic rhinosinusitis by activating the ERK/STAT3 pathway

Haotian Wu<sup>#</sup>, Yue Li<sup>#</sup>, Xia Li<sup>#</sup>, Weiqiang Huang, Zizhen Huang, Xiaoping Lai, Junming Ma, Yanjie Jiang, Yana Zhang, Lihong Chang<sup>\*</sup>, Gehua Zhang<sup>\*</sup>

Rhinology 62: 6, 726 - 738, 2024  
<https://doi.org/10.4193/Rhin24.127>

## IL-17A disrupts the nasal mucosal epithelial barrier in patients with chronic rhinosinusitis by activating the ERK/STAT3 pathway



Wu H, Li Y, Li X, et al. Rhinology 2024. <https://doi.org/10.4193/Rhin24.127>

### Abstract

**Background:** The mucosal epithelial barrier, the first line of immune defense, is vulnerable to allergens, pathogens, and inflammatory cytokines, contributing to CRS development. Our previous studies found high interleukin-17A (IL-17A) expression correlated with CRS severity and low glucocorticoid efficacy. The role of IL-17A in disrupting the nasal mucosal epithelial barrier leading to CRS remains unclear. We aimed to investigate how IL-17A promoting epithelial barrier damage and identify new treatment targets for CRS.

**Methodology:** Nasal tissue samples from 36 CRSwNP, 34 CRSsNP, and 39 controls were examined for the expression of IL-17A and tight junction (TJ) proteins using qRT-PCR, immunohistochemistry and immunofluorescence. The integrity of TJs and signaling pathways activation were observed using western blot, immunofluorescence, TEER and FITC-FD4, transmission electron microscopy before and after IL-17A stimulation in human primary nasal epithelial cells (hNECs). Concurrently, studies were also conducted in an CRS mouse model induced by anti-IL-17A neutralizing antibody administration.

**Results:** TJs expression in the nasal mucosa of CRS patients was lower than in controls. IL-17A stimulation reduced TJs expression and TEER while increasing hNECs permeability. Inhibition of the (ERK/STAT3) pathway reversed the downregulation of TJs and the disruption of the epithelial barrier induced by IL-17A stimulation. In the CRS mouse model, anti-IL-17A antibody treatment rescued the nasal mucosal epithelial barrier.

**Conclusions:** IL-17A disrupts the nasal mucosal epithelial barrier by activating the ERK/STAT3 pathway in patients with CRS.

**Key words:** chronic rhinosinusitis, interleukin-17a, epithelial barrier, tight junction

## Introduction

Chronic rhinosinusitis (CRS) is a prevalent chronic inflammatory disease of the upper respiratory tract, affecting approximately 8% of the population in China<sup>(1-3)</sup>. It is a heterogeneous disease characterized by persistent inflammation in the upper respiratory tract and nasal sinuses, leading to a significant reduction in quality of life<sup>(4)</sup>. The pathogenesis and treatment of CRS are currently the major areas of focus in rhinology research<sup>(5-7)</sup>.

The epithelial barrier serves as the first line of defense in the human immune system<sup>(8)</sup>. Numerous studies have demonstrated that disruption of this barrier plays a vital role in chronic inflammatory airway diseases<sup>(9)</sup>. Tight junctions, which are located on the most apical side of the lateral membrane of epithelial cells, are critical components of the epithelial barrier<sup>(10)</sup>.

Rogers et al. and Meng et al. found that the expression of tight junction (TJ) proteins was downregulated in the nasal polyps of patients with chronic rhinosinusitis with nasal polyps (CRSwNP) compared to healthy nasal mucosa<sup>(11,12)</sup>. Similarly, Soyka et al. found that the mRNA expression levels of claudin-4 and occludin were downregulated in the nasal polyps of CRSwNP patients compared to those in patients with chronic rhinosinusitis without nasal polyps (CRSsNP) and healthy controls<sup>(13)</sup>. They also found that the continuous expression of occludin in the apical lateral membrane of epithelial cells was destroyed in CRS patients<sup>(13)</sup>. These findings highlight the dysfunction of the epithelial barrier in CRS.

When the epithelial barrier is damaged, pathogens can translocate to interepithelial and deeper subepithelial locations through the leaky epithelial barrier, leading to inflammatory reactions. Local inflammation reduces the expression of TJs and exacerbates damage to the epithelial barrier. This allows more pathogens to penetrate the epithelial barrier, promoting persistent inflammation and thereby exacerbating the disease<sup>(5,13,14)</sup>. Our previous study showed that IL-17A is highly expressed in the nasal mucosa of patients with CRS, especially those with CRSwNP, and contributes to the resistance of CRS to glucocorticoid therapy<sup>(15)</sup>. Recent studies have shown that IL-17A is associated with a decrease in claudin-1 and disruption of the inherent barrier, leading to bacterial infiltration that induces intestinal inflammation<sup>(16)</sup>. IL-17A blocking effectively reduced intestinal mucosal epithelial barrier disruption and alleviated intestinal mucosal inflammation in a burn mouse model<sup>(17)</sup>. However, further investigation is required to determine whether IL-17A disrupts the nasal mucosal epithelial barrier in patients with CRS, thereby exacerbating nasal mucosal inflammation. In this study, we explored the role of IL-17A in regulating the nasal mucosal epithelial barrier. These results provide new insights into the pathogenesis of CRS and identify potential therapeutic targets.

## Materials and methods

### Subjects and samples

This study was approved by the Ethics Committee of the Third Affiliated Hospital of Sun Yat-Sen University (Approval No. [2016]2-26). CRSsNP and CRSwNP were diagnosed and classified according to the EPOS 2020 guidelines<sup>(4)</sup>. More detailed descriptions on subject characteristics are provided in Supplementary Material section, Table S1 and, Table S2.

### Immunohistochemistry and immunofluorescence

The levels of expression of IL-17A, TJs, and signal pathway proteins were evaluated by using immunofluorescence and immunohistochemistry. For more detail, please see the Supplementary Material section.

### qRT-PCR

Quantitative real-time PCR (qRT-PCR) assay was conducted as previously described<sup>(18)</sup>. Relative gene expression was calculated using the  $2^{-\Delta\Delta Ct}$  method. The primers used for qRT-PCR are described in Table S3.

### Air-liquid interface (ALI) culture and treatment of hNECs

The single-cell suspensions of hNECs prepared from nasal polyps, as previously described<sup>(15)</sup>, were resuspended in EX-PLUS culture medium (STEMCELL) and seeded into the upper chamber of 24-well Transwell plates at an approximate concentration of  $2 \times 10^4$  cells in 200  $\mu$ L of EX-PLUS culture medium per well. In addition, 500  $\mu$ L of EX-PLUS culture medium was added to the lower chamber. The cells were cultured until they reached nearly 100% confluence. At this point, the medium in the lower chamber was replaced with 500  $\mu$ L of ALI culture medium (STEMCELL). The medium was changed every other day, and ciliary differentiation of hNECs was observed under an inverted microscope. After 14 days of culture, the culture medium in the lower chamber was replaced with ALI culture medium containing 500 ng/mL of anti-IL-17A neutralizing antibody, 20  $\mu$ mol/mL of PD98059 (PD, an ERK inhibitor), or 10  $\mu$ mol/mL of Cryptotanshinone (CRY, a STAT3 inhibitor). After 1 hour, 300 ng/mL of recombinant human IL-17A was added to the corresponding lower chamber, and the cells were cultured for an additional 24 hours. For the control group, the medium was replaced with freshly prepared ALI culture medium. In the inhibitor control group, the medium was replaced with an ALI culture medium containing a 1:500 dilution of DMSO.

### Measurement of trans-epithelial electrical resistance (TEER) and cell permeability

Cells cultured on Transwell filters for 14 days were subjected to different treatments. TEER was measured using a Millicell<sup>®</sup> ERS-2 (Electrical Resistance System). The Millicell<sup>®</sup> ERS-2 system was first calibrated to zero in a freshly prepared ALI medium,

and then the positive and negative poles were inserted into the upper and lower chambers, respectively, to record the resistance value of each well. For measuring epithelial cell permeability, both chambers were washed three times with DPBS and then were added with 4kDa FITC-FD4 solution (10 mg/mL in 400  $\mu$ L PBS to the upper chamber). After culturing for 180 min, a 100- $\mu$ L aliquot of PBS was collected from the lower chamber for the concentration measurement of FITC-dextran by using a microplate reader (Tecan Spark 10M). The cell permeability rate was represented as the quality of FITC-dextran per square centimeter of the transwell filters per minute.

### Western blotting

Western blotting was performed according to previously described methods<sup>(19)</sup>.

### Transmission electron microscopy

The prepared hNECs cultured in Transwell filters were fixed in 3% glutaraldehyde and incubated at 4°C overnight. The following day, the cells were dehydrated using a graded series of ethanol concentrations. After dehydration, the cells were embedded in Embed 812 resin and cut into 60-nm-thick sections. The sections were stained with 2.0% uranyl acetate and 2.0% lead citrate solutions. The cells were observed and imaged using a transmission electron microscope.

### Mouse model

Female BALB/c mice (aged 6–8 weeks, 18–20 g weight) were acquired and randomly divided into four groups: control, experimental chronic rhinosinusitis (ECRS), ECRS + anti-IL-17A neutralization group, and ECRS + IL-17A stimulation ( $n = 5$  in each group). The detailed treatments for each group are described in our previous study<sup>(20)</sup>.

### Statistical analysis

Statistical analysis was conducted using SPSS version 25.0 (IBM, Armonk, NY, USA), and statistical significance was defined as  $p < 0.05$ . Data are presented as the mean  $\pm$  standard deviation or median  $\pm$  interquartile range, according to it corresponds to normal distribution or not. When comparisons were made among groups, the Kruskal-Wallis H test was used to assess significant intergroup variability. Mann-Whitney U or Student t tests were used for between-group comparisons. Correlation analysis was performed using the Pearson correlation test. Binary data were analyzed using the chi-squared test. All statistical figures were generated using GraphPad Prism version 8.02.

## Results

### Expressions of IL-17A and tight junction proteins in the nasal mucosal tissue of patients with chronic rhinosinusitis

As shown in Figures 1A and 1B, IL-17A was expressed in both the

epithelium and stroma of nasal mucosal, whereas the expressions of claudin-1, occludin, and ZO-1 were mainly observed in the epithelial cells. The expression of IL-17A was obviously increased in the nasal mucosal of patients with CRSwNP and CRSsNP compared to controls ( $p < 0.01$  for all), whereas the expressions of claudin-1, occludin, and ZO-1 were lower in the nasal mucosal from patients with CRSwNP and CRSsNP compared to controls ( $p < 0.01$  for all). The expressions of IL-17A and ZO-1 were significantly higher in the nasal mucosal of patients with CRSwNP compared to those with CRSsNP ( $p < 0.01$ ). The expressions of claudin-1, occludin, and ZO-1 were lower in the nasal mucosal of patients with CRSwNP compared to those with CRSsNP, but the differences were not statistically significant ( $p > 0.05$ ). As shown in Figure 1C, the mRNA expressions of claudin-1, occludin, and ZO-1 were significantly lower in the nasal mucosal of patients with CRSwNP compared to controls ( $p < 0.05$  for all). The mRNA expression of claudin-1 was also decreased in patients with CRSsNP compared to controls, although this difference was not statistically significant ( $p > 0.05$ ). The mRNA expressions of occludin and ZO-1 were lower in the nasal mucosal of patients with CRSsNP compared to controls ( $p < 0.05$  for both).

### Localization and correlation analysis of IL-17A and tight junction proteins in nasal mucosal tissues of patients with chronic rhinosinusitis

As shown in Figures 2A–2F, it was confirmed that IL-17A was expressed in both the epithelial cells and sub-epithelial stroma of nasal mucosal, while claudin-1, occludin, and ZO-1 were mainly expressed in the epithelial cells of the nasal mucosa. The expression of IL-17A was increased in the epithelial cells from both patients with CRSwNP and CRSsNP compared to controls ( $p < 0.01$  for all), while the expressions of claudin-1, occludin, and ZO-1 were lower in nasal mucosal from patients with CRSwNP and CRSsNP compared to controls ( $p < 0.01$  for all). The expression of IL-17A in the nasal mucosal epithelium was negatively correlated with the expressions of claudin-1, occludin, and ZO-1 in all groups, with correlation coefficients of -0.9340, -0.8815, and -0.8807, respectively ( $p < 0.01$ ; Figure 2G).

### IL-17A disrupted the epithelial barrier in hNECs

As demonstrated in Figures 3A–3D, IL-17A stimulation reduced the expression of TJs claudin-1, occludin, and ZO-1 in hNECs cultured using an ALI method ( $p < 0.01$  for all). IL-17A stimulation combined with anti-IL-17A antibody neutralization could reverse the IL-17A-induced decrease in TJs ( $p < 0.05$  for all). Transmission electron microscopy revealed that the gap between cells was increased in the most apical side of the lateral membrane of the IL-17A-stimulated ALI-cultured hNECs. However, these enlarged gaps in hNECs treated with IL-17A stimulation combined with anti-IL-17A antibody neutralization (Figure 3E). The counts of cells with enlarged gaps at the most apical side of the lateral

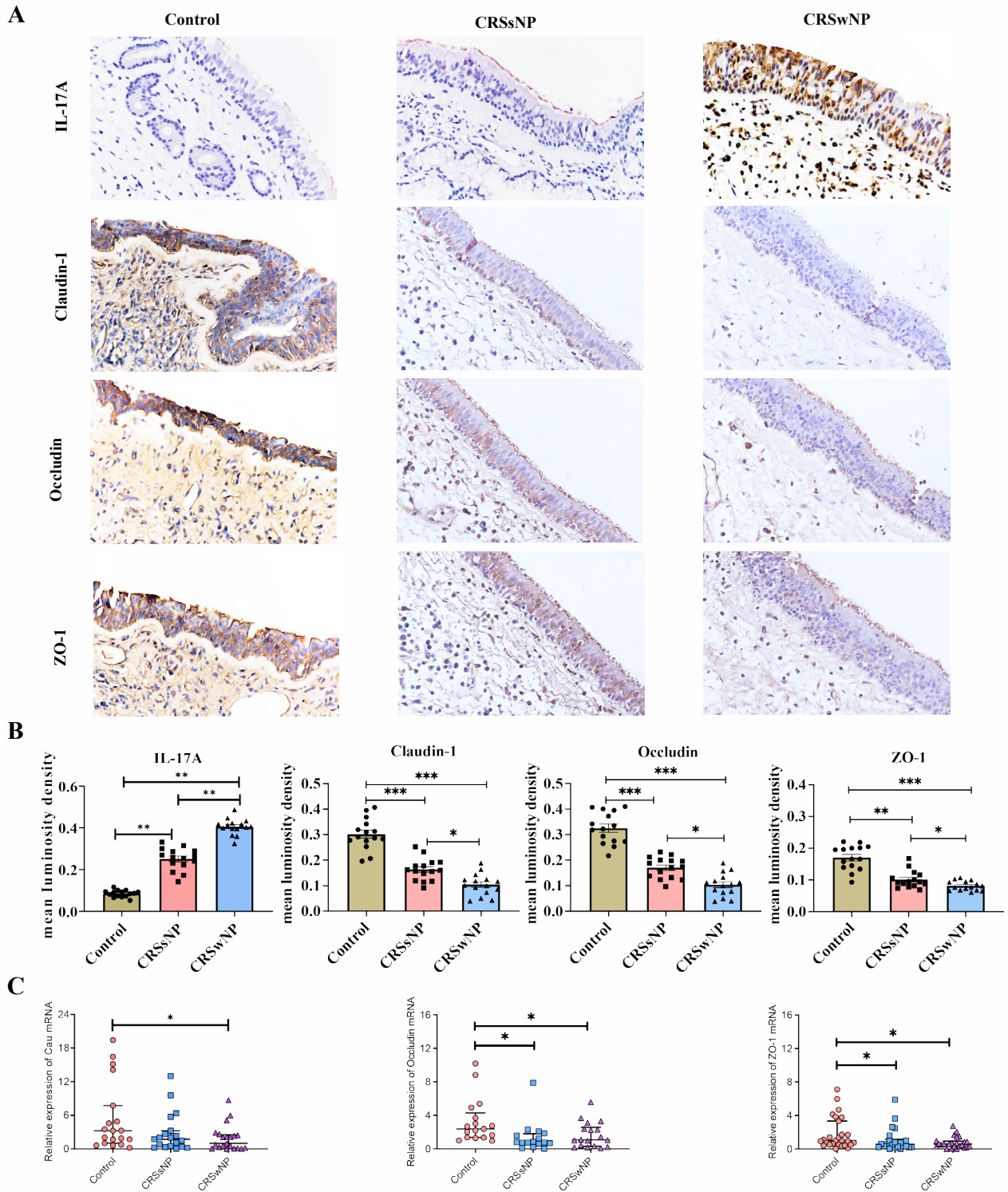


Figure 1. Expressions of IL-17A and tight junction proteins in the nasal mucosal tissues of patients with chronic rhinosinusitis and healthy controls. A) Representative immunohistochemistry images of the expressions of IL-17A and tight junction proteins (claudin-1, occludin, and ZO-1) in the nasal mucosal tissues of the controls and patients with CRSsNP and CRSwNP. B) Quantitative analysis of the expressions of tight junction proteins and IL-17A in the nasal mucosal tissues of the controls and patients with CRSsNP and CRSwNP. Data presented as means  $\pm$  SEMs. C) Quantitative analysis of mRNA expressions of claudin-1, occludin, and ZO-1 in the nasal mucosal tissues of the controls and patients with CRSsNP and CRSwNP. Mann-Whitney test. \* $p < 0.05$ , \*\* $p < 0.01$ , \*\*\* $p < 0.001$ . Immunohistochemistry (400 $\times$  magnification). Figure 1A and B, 15 nasal tissue sample in each group. Figure 1C, control subjects,  $n = 19-27$ ; patients with CRSsNP,  $n = 16-22$ ; patients with CRSwNP,  $n = 18-25$ .

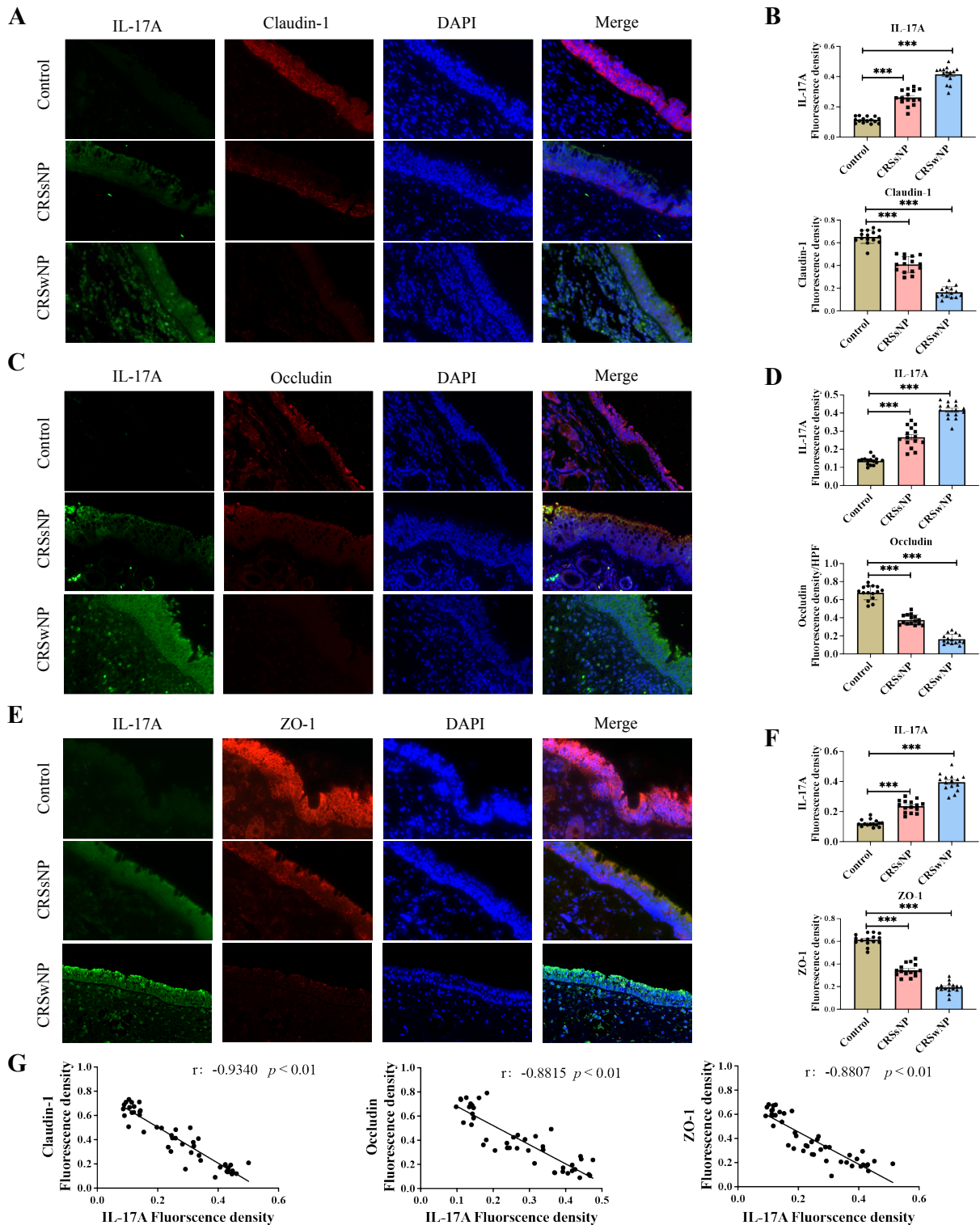


Figure 2. Location and correlation of IL-17A and tight junction proteins in nasal mucosal tissues of patients with CRS and healthy controls. A and B) Representative immunofluorescence image and quantitative analysis of the expressions of IL-17A and claudin-1 in nasal mucosal tissues of controls and patients with CRSsNP and CRSwNP. C and D) Representative immunofluorescence image and quantitative analysis of the expressions of IL-17A and occludin in nasal mucosal tissues of controls and patients with CRSsNP and CRSwNP. E and F. Representative immunofluorescence image and quantitative analysis of the expressions of IL-17A and ZO-1 in nasal mucosal tissues of controls and patients with CRSsNP and CRSwNP. G. Correlation analysis of IL-17A with claudin-1, occludin, and ZO-1. Data presented as means  $\pm$  SEMs. \* $p < 0.05$ , \*\* $p < 0.01$ , \*\*\* $p < 0.001$ . Immunofluorescence (400 $\times$  magnification). Figure 2A-F, 15 nasal tissue sample in each group.

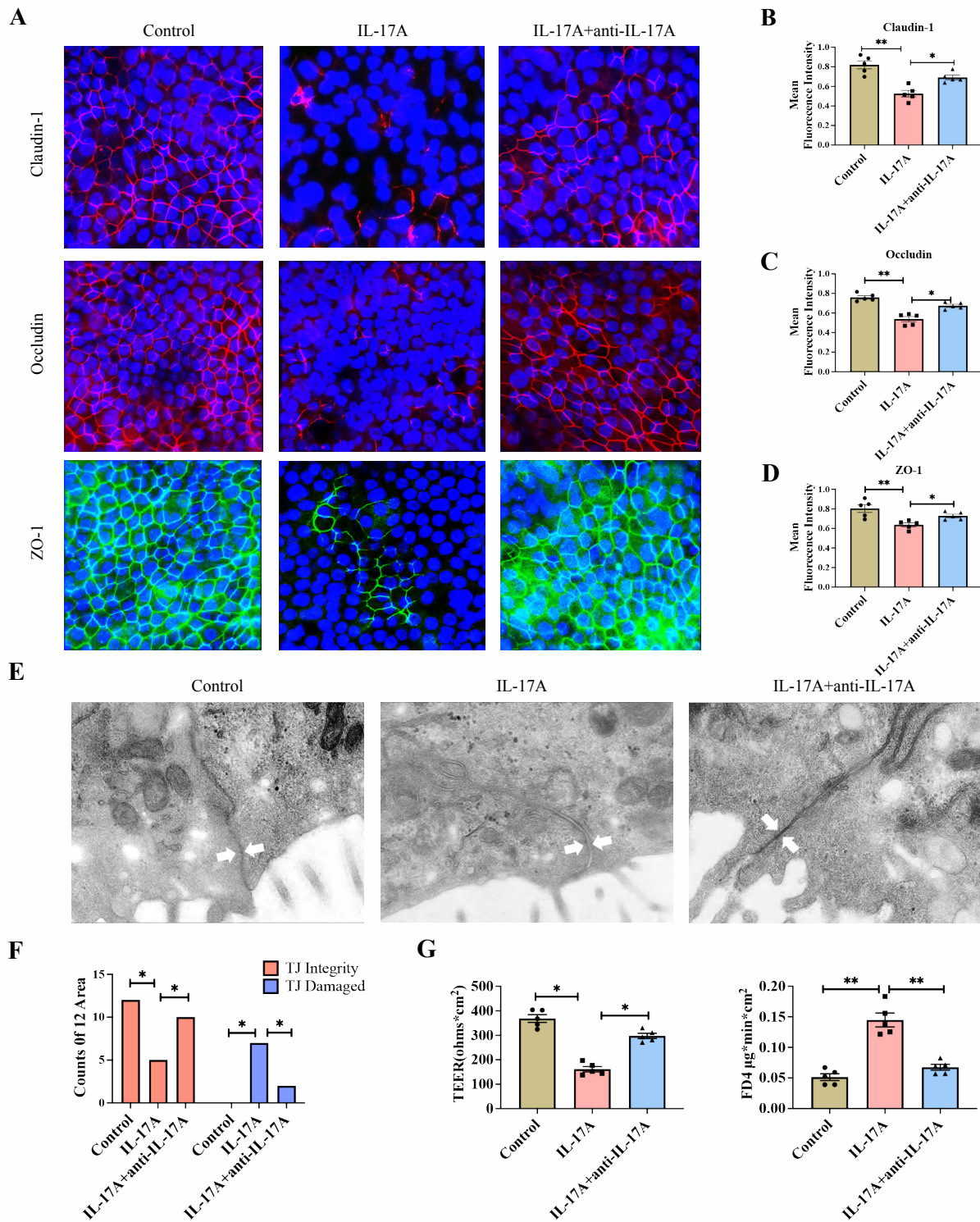


Figure 3. IL-17A downregulated tight junction proteins expression and disrupted epithelial barrier integrity in hNECs. A) Immunofluorescence staining of tight junction protein expressions in hNECs cultured in ALI after different treatments (confocal microscopy 630×). B–D) Quantitative analysis of expressions of claudin-1, occludin, and ZO-1 in hNECs cultured in ALI with different treatments. E and F) Representative transmission electron micrographs and quantitative analysis of tight junctions of hNECs with different treatments after 24 hours (5000× magnification) G) TEER and FD4 permeability experiments to assess transmembrane resistance and permeability in hNECs cultured in ALI with different treatments. Data presented as means ± SEMs. \*p < 0.05, \*\*p < 0.01, \*\*\*p < 0.001. White arrow indicates the tight junction. Figure 3A–D, and G, 5 biopsy specimens in each group.

membrane was increased in hNECs treated with IL-17A stimulation compared to the control. These changes could be effectively reversed by anti-IL-17A antibody neutralization ( $p < 0.05$  for all; Figure 3F). Moreover, the TEER was decreased while the permeability was increased in the hNECs with IL-17A stimulation compared to the controls. These damages were reversed in hNECs treated with anti-IL-17A antibody neutralization (Figure 3G,  $p < 0.05$ ).

#### **IL-17A disrupted the epithelial barrier through activating the ERK/STAT3 signaling pathway in hNECs**

As shown in Figures 4A and 4B, IL-17A stimulation increased the expression of phosphorylated ERK (p-ERK) and phosphorylated STAT3 (p-STAT3) in hNECs ( $p < 0.01$  for both). Treatment with the ERK inhibitor PD significantly reversed the increased expression of p-ERK in IL-17A-stimulated hNECs. Similarly, STAT3 pathway inhibition with CRY reversed the increased expression of p-STAT3 induced by IL-17A stimulation ( $p < 0.01$  for both; Figures 4C–4G). As demonstrated in Figures 4H–4K, blocking the ERK pathway inhibited IL-17A-induced upregulation of p-ERK and p-STAT3 ( $p < 0.05$  for both). However, blocking the STAT3 pathway only inhibited the IL-17A-induced upregulation of p-STAT3, but did not inhibit IL-17A-induced upregulation of p-ERK.

The expressions of claudin-1, occludin, and ZO-1 were decreased in hNECs treated with IL-17A compared to the control group ( $p < 0.01$  for all). This decrease in the three TJ proteins was reversed in hNECs treated with IL-17A stimulation combined with ERK or STAT3 inhibitors ( $p < 0.05$  for all; Figures 5A and 5B). Transmission electron microscopy results showed that IL-17A stimulation widened intercellular gaps and disrupted TJ structures in hNECs ( $p < 0.05$  for both). The widened intercellular gaps and disrupted TJ structures in hNECs treated with IL-17A combined with ERK (PD) or STAT3 inhibitor (CRY) were alleviated when compared to those in IL-17A-treated hNECs (Figures 5C and 5D). In addition, IL-17A stimulation significantly reduced the TEER and increased the permeability of hNECs ( $p < 0.01$  for both). Both ERK and STAT3 inhibition could reverse the IL-17A-induced decrease in transmembrane resistance and increase in permeability of hNECs ( $p < 0.05$  for all; Figures 5E and 5F).

#### **IL-17A disrupted the epithelial barrier in mouse nasal mucosal**

As shown in Figures 6A and 6B, an increase in IL-17A expression and a decrease in claudin-1 expression were observed in the nasal mucosal epithelium of the ECRS mice when compared to the control mice ( $p < 0.01$  for both). ECRS mice treated with IL-17A stimulation (ECRS + IL-17A) showed higher IL-17A expression but lower claudin-1 expression in the nasal mucosa compared to ECRS mice, while the ECRS mice treated with anti-IL-17A antibody blocking (ECRS + anti-IL-17A) showed lower IL-17A expression but higher claudin-1 expression in the nasal

mucosal epithelium compared to ECRS mice ( $p < 0.05$  for all). As demonstrated in Figures 6C–6F, the expressions of occludin and ZO-1 were also lower in the nasal mucosal epithelium of ECRS mice compared to control mice. ECRS mice treated with IL-17A stimulation (ECRS + IL-17A) showed higher IL-17A expression but lower occludin and ZO-1 expressions in the nasal mucosa compared to ECRS mice, while the ECRS mice treated with anti-IL-17A antibody blocking (ECRS+anti-IL-17A) showed lower IL-17A expression but higher occludin and ZO-1 expressions in the nasal mucosal epithelium compared to ECRS mice ( $p < 0.05$  for all).

#### **Discussion**

Disruption of the epithelial barrier is a critical characteristic of many chronic inflammatory diseases<sup>(9,21)</sup>. Impaired barrier function leads to increased epithelial permeability, which further exacerbates inflammation and epithelial barrier damage<sup>(22)</sup>. TJ are the most important structures in the nasal mucosal epithelial barrier formation, and are composed of the claudin family, occludin, and ZO-1 proteins<sup>(23)</sup>. In this study, we found that the expression of TJs was the lowest in the nasal mucosa of patients with CRSwNP. This finding is consistent with previous studies by Rogers et al. and Meng et al.<sup>(11,12)</sup>. This implies that the damage to the nasal epithelial barrier in patients with CRS, especially those with CRSwNP, may be disrupted by a decrease in TJs. An increasing number of studies have shown that patients with CRSwNP are predominantly characterized by type1/type3 inflammation in Asians and that IL-17A plays an important role in CRS<sup>(18,24,25)</sup>. Rha et al. conducted a study in Korean patients with CRS and found that IL-17A expression was significantly increased in patients with CRSwNP and correlated with the severity of the condition<sup>(26)</sup>. Our previous studies also found an increase in IL-17A levels in the nasal mucosa of patients with CRSwNP<sup>(19)</sup>, which worsened CRS symptoms<sup>(15)</sup>. Song et al. reported that IL-17A is associated with intestinal epithelial barrier disruption<sup>(17)</sup>. These findings suggest that high IL-17A expression may be involved in epithelial barrier disruption and the occurrence of CRSwNP. In this study, we found that an increase in IL-17A levels negatively correlated with a decrease in TJs in the nasal mucosal epithelium. This finding suggests that IL-17A is associated with a reduction in the expression of TJs.

Previous studies have reported that when cultured on permeable supports in air-liquid interface (ALI) culture, epithelial cells can differentiate into pseudostratified epithelia, recapitulating the features of the human airway epithelium in vivo<sup>(27-29)</sup>. Consequently, ALI cultures are widely used in airway research<sup>(5,28)</sup>. Studies have shown that epithelial cells cultured in ALI can form a complete epithelial barrier<sup>(30)</sup>. When the epithelial barrier is disrupted, TEER decreases and FD4 permeability increases<sup>(30)</sup>. In this study, we found that IL-17A stimulation reduced TEER and increased the permeability of ALI-cultured hNECs, along

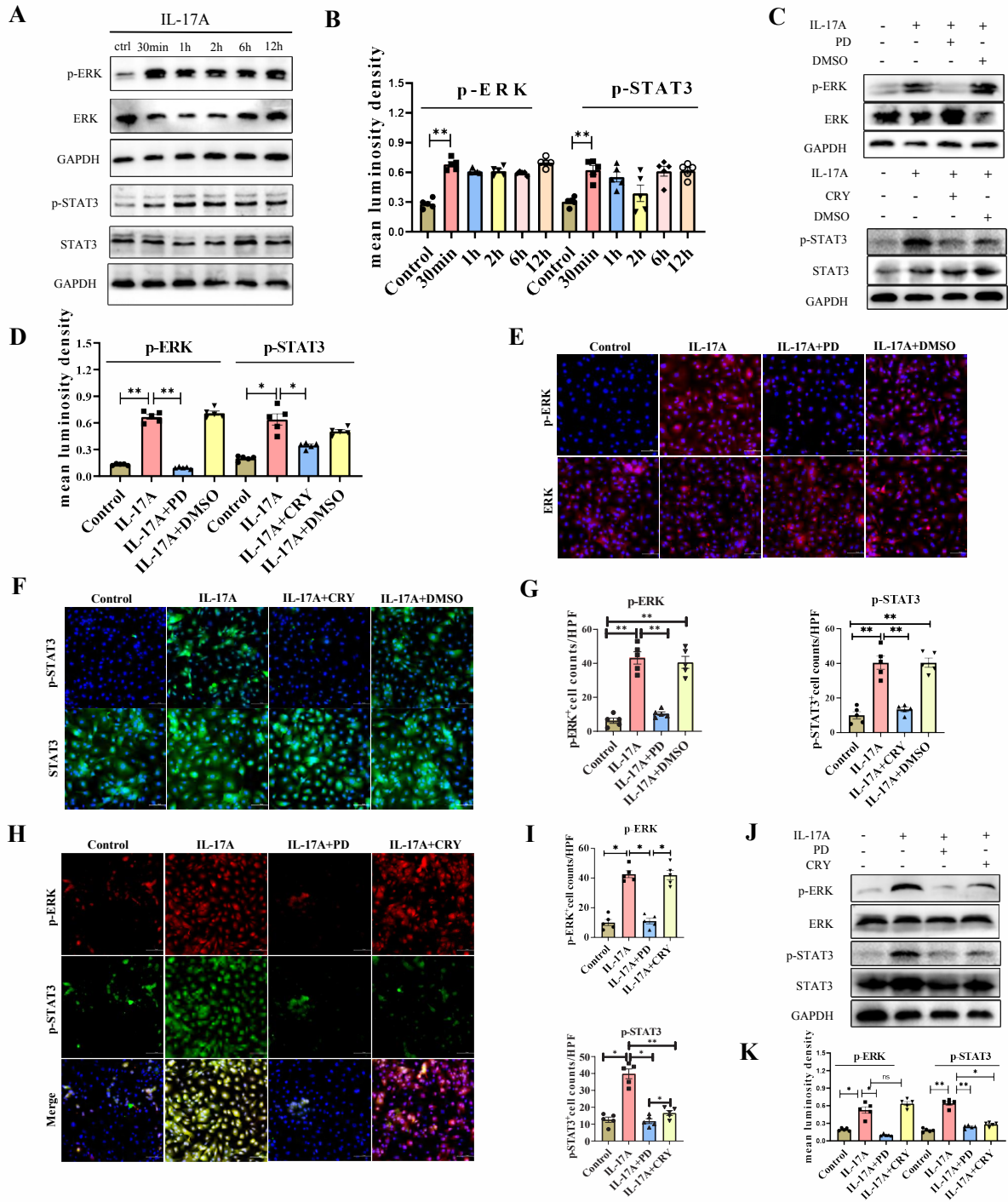


Figure 4. IL-17A activates the ERK/STAT3 signaling pathway. A and B) Western blot analysis and quantitative analysis of p-ERK and p-STAT3 expression in hNECs with 300 ng/mL IL-17A stimulation at different time points. C) Western blot analysis of p-ERK and ERK expressions in hNECs with and without IL-17A stimulation alone, IL-17A combined with PD or DMSO, and western blot analysis of p-STAT3 and STAT3 expressions in hNECs with and without IL-17A stimulation, IL-17A combined with CRY or DMSO. D) Quantitative analysis of western blot of p-ERK and p-STAT3 in hNECs with different treatments. E) Immunofluorescence staining of p-ERK and ERK expressions in hNECs with and without IL-17A stimulation, IL-17A combined with PD or DMSO. F) Immunofluorescence staining of p-STAT3 and STAT3 expressions in hNECs with and without IL-17A stimulation, IL-17A combined with CRY or DMSO. G) Quantitative analysis of immunofluorescence staining of p-ERK and p-STAT3 expressions in hNECs with different treatments. H and I) Immunofluorescence staining and quantitative analysis of p-ERK and p-STAT3 in control, IL-17A stimulation, IL-17A combined with PD and IL-17A combined with CRY. J and K) Western blot analysis and quantitative analysis of p-ERK and p-STAT3 in control, IL-17A stimulation, IL-17A combined with PD and IL-17A combined with CRY. PD: inhibitor of ERK pathway. CRY: inhibitor of STAT3 pathway. Data presented as means  $\pm$  SEMs. \* $p < 0.05$ , \*\* $p < 0.01$ , \*\*\* $p < 0.001$  Figure 4A-K, 5 biopsy specimens in each group.

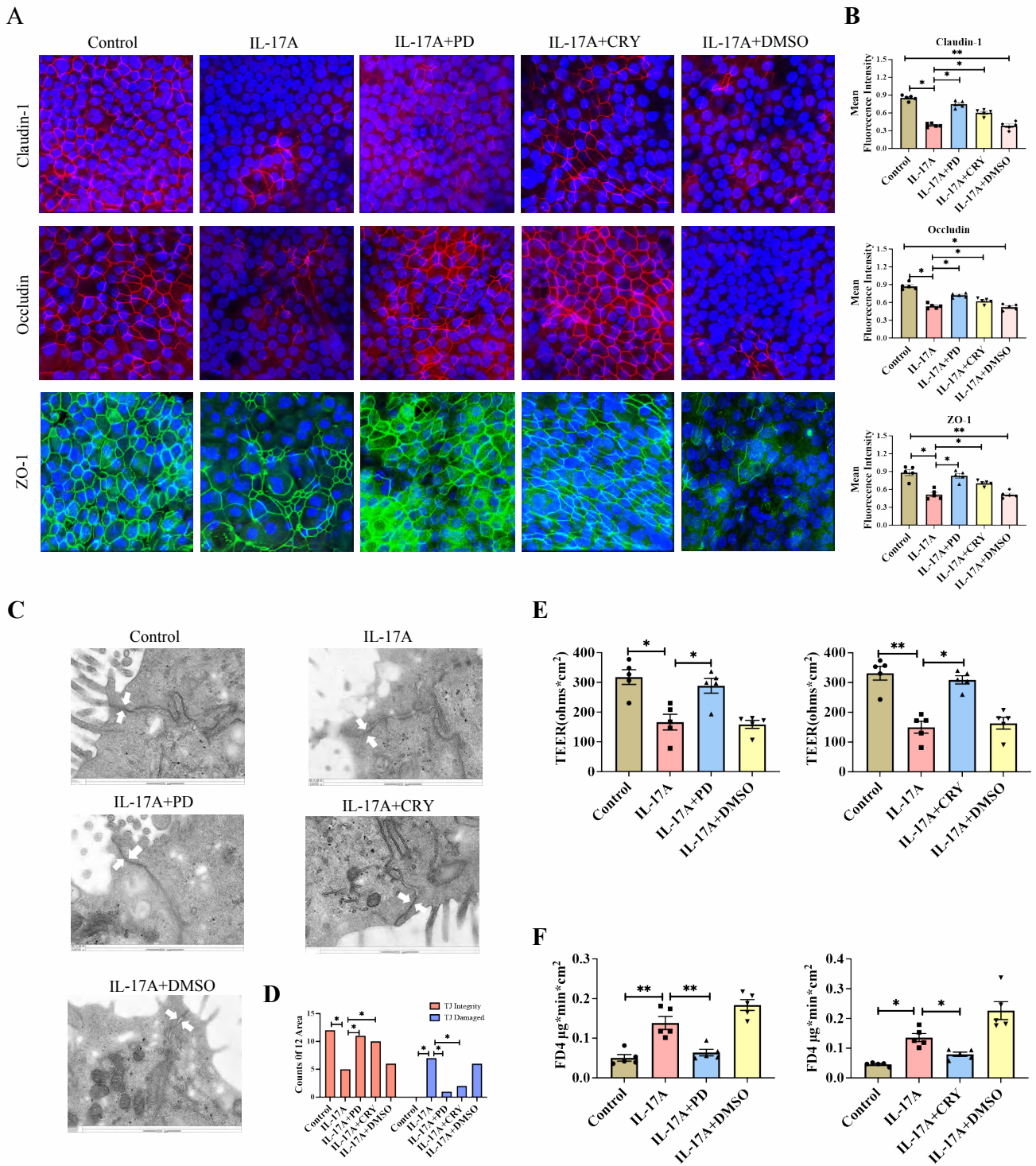


Figure 5. IL-17A downregulated the expressions of tight junction proteins and disrupted the epithelial barrier integrity by activating the ERK/STAT3 signaling pathway in ALI-cultured hNECs. A and B) Immunofluorescence staining and quantitative analysis of tight junction proteins (claudin-1, occludin, ZO-1) in hNECs cultured with ALI after different treatments (confocal microscopy; 630× magnification). C) Representative transmission electron micrographs of hNECs cultured with ALI after different treatments for 24 hours. (5000× magnification). D) Quantitative analysis of tight junction in hNECs cultured with ALI after different treatments for 24 hours under transmission electron micrographs. E) TEER measurement in ALI-cultured hNECs with different treatments. F) FD4 permeability assay to assess permeability in ALI-cultured hNECs with different treatment. Data presented as means ± SEMs. \*p < 0.05, \*\*p < 0.01, \*\*\*p < 0.001. White arrow indicates the tight junction. PD: inhibitor of ERK pathway. CRY: inhibitor of STAT3 pathway. Figure 5A-B and E-F, 5 biopsy specimens in each group.

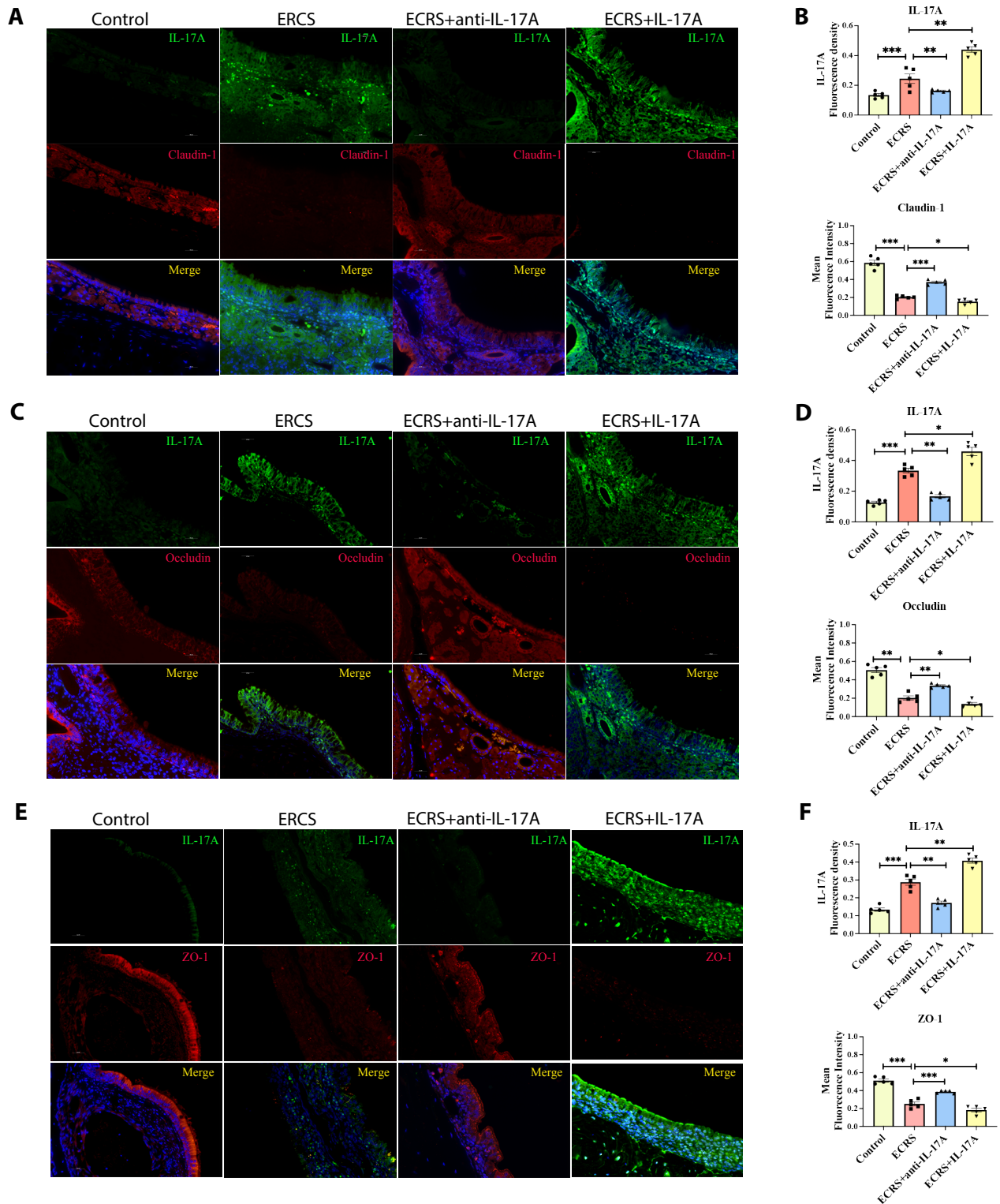


Figure 6. IL-17A downregulated the expressions of tight junction proteins in mouse nasal sinus mucosal. A and B) Immunofluorescence staining and quantitative analysis of IL-17A and tight junction protein claudin-1 expression in the mouse nasal sinus mucosa in various groups. C and D) Immunofluorescence staining and quantitative analysis of IL-17A and tight junction protein occludin in the mouse nasal sinus mucosa in various groups. E and F) Immunofluorescence staining and quantitative analysis of IL-17A and tight junction protein ZO-1 in the mouse nasal sinus mucosa in various groups. Data presented as means  $\pm$  SEMs. \* $p < 0.05$ , \*\* $p < 0.01$ , \*\*\* $p < 0.001$ . Immunofluorescence (400x magnification). Figure 6A-F, control subjects,  $n = 5$ ; ECRS,  $n = 5$ ; ECRS+anti-IL-17A,  $n=5$ ; ECRS+ IL-17A,  $n=5$ .

with the downregulation of TJs in hNECs. Moreover, IL-17A stimulation increased the gap between the cells, as detected by transmission electron microscopy. However, these effects were mitigated by neutralization with an anti-IL-17A antibody. This result is consistent with Li et al.'s finding that IL-17A downregulates the expression of TJs in the intestinal mucosa of mice with ulcerative colitis<sup>(31)</sup>. Mahnaz et al. found that IL-17A can lead to decreased TEER and increased permeability of nasal mucosal epithelial cells, as well as discontinuous expression of zonula occludens-1 (ZO-1)<sup>(32)</sup>. These findings support the hypothesis that IL-17A disrupts the epithelial cell barrier by inhibiting the expression. However, the specific mechanism by which IL-17A reduces the expression remains unclear.

Recent studies have demonstrated that IL-17A activates the ERK signaling pathway, increases skin keratinocyte inflammation, and exacerbates psoriasis<sup>(33)</sup>. IL-17A has also been shown to activate the STAT3 signaling pathway, disrupt mouse corneal epithelium, worsen dry eye symptoms<sup>(34)</sup>. These findings suggest that IL-17A exerts its biological effects by activating both ERK and STAT3 signaling pathways. In this study, we observed that the expression of p-ERK and p-STAT3 in hNECs significantly increased after IL-17A stimulation, indicating activation of the ERK and STAT3 signaling pathways. Further experiments revealed that IL-17A initially activates the ERK signaling pathway, followed by the activation of the STAT3 pathway. Subsequently, this process inhibits the expression of TJs and disrupts the nasal mucosal epithelial barrier.

ALI-cultured hNECs are not fully comparable to the pathophysiological phenomena in humans due to their lack of interaction with the environment *in vivo*, for example the impacts of inflammatory cells, fibroblasts, or other types of cells in the subepithelial stroma, and the influence of pathogens or allergens in the airways. Hence, to elucidate whether IL-17A disrupts the epithelial barrier *in vivo*, we established an eosinophilic chronic rhinosinusitis (ECRS) mouse model that exhibits typical CRS histopathological changes in the nasal cavity and sinuses<sup>(35,36)</sup>. We found that IL-17A stimulation decreased the expression in mouse nasal mucosa and disrupted its structural integrity. These findings were consistent with our results *in vitro*. Intraperitoneal injection of IL-17A-neutralizing antibodies in ECRS mice increased the expression of nasal mucosal TJs and restored their structural integrity. This was supported by the finding that intraperitoneal injection of IL-17A-neutralizing antibodies increased the expression of the ZO-1 and reversed the disruption of the epithelial barrier in the intestinal mucosa and retina of mice<sup>(37,38)</sup>. Numerous studies have shown that disruption of the epithelial barrier exacerbates chronic inflammation and is closely associated with the development of various inflammatory diseases<sup>(39,40)</sup>. Our previous study showed that the intraperitoneal injection of IL-17A-neutralizing antibodies alleviated nasal mucosal inflammation in ECRS mice<sup>(20)</sup>. In this study, we showed that IL-17A

induces a reduction in the expression of TJs in ECRS mice. Our findings suggest that IL-17A leads to nasal epithelial barrier dysfunction, which contributes to the pathogenesis of ECRS. However, these findings did not support the hypothesis that IL-17A exacerbates nasal mucosal inflammation by disrupting the epithelial barrier. Further studies involving TJs knockout mice or mice overexpressing these proteins are needed to more definitively illustrate whether IL-17A worsens nasal mucosal inflammation by disrupting the epithelial cell barrier.

IL-17A monoclonal antibodies have been used in clinical practice for several years and have proven effective in treating diseases. In a comprehensive analysis of 21 clinical trials using the IL-17A monoclonal antibody for the treatment of psoriasis, ankylosing spondylitis, and psoriatic arthritis, the IL-17A monoclonal antibody showed a significant therapeutic effect compared to the placebo group<sup>(41)</sup>. However, studies have shown that the use of IL-17A monoclonal antibodies may cause clinical side effects, particularly increasing the risk of infection with long-term use<sup>(42,43)</sup>. Hence, we aim to extend our study and detect systemic inflammation in mice to test the safety and tolerance of anti-IL-17A monoclonal antibodies (mAbs) *in vivo*.

In addition to studying the effects of the type 3 cytokine IL-17A, we investigated how the type 1 cytokine interferon-gamma IFN- $\gamma$  and type 2 cytokines (IL-4 and IL-13) impact the epithelial barrier. Consistent with previous studies<sup>(13,44)</sup>, we found that IFN- $\gamma$ , IL-4, and IL-13 decreased TEER and TJ expression while increasing the permeability of hNECs (Supplement Figure S2). In addition to inflammatory factors, physical conditions such as atopy are associated with CRS pathogenesis<sup>(45)</sup>. Vijay et al. found that increased expression of small proline-rich proteins, which are predictors of asthma development, leads to epithelial barrier dysfunction in CRS patients with allergic rhinitis (AR)<sup>(46)</sup>. However, the limited number of patients with atopic dermatitis in our study made statistical analysis difficult. The relationship between atopy and the nasal mucosal epithelial barrier thus requires further investigation. Lifestyle factors, such as smoking, are also associated with CRS development<sup>(45)</sup>. Heijink et al. found that cigarette smoke extract reduced epithelial integrity<sup>(47)</sup>. However, in this study, nasal mucosal samples from smokers and non-smokers showed no significant differences in TJs expression (Supplement Figure S1). This could be due to the insufficient number of patients or the need for a more accurate sub-classification of daily smoking quantity to reflect its actual impact on the epithelial barrier, as Zhang et al. found a correlation between chronic rhinosinusitis incidence and daily cigarette consumption<sup>(48)</sup>.

## Conclusion

This study found that IL-17A reduced the expression of TJ proteins in the nasal mucosal epithelium both *in vitro* and *in vivo*, which was associated with the activation of the ERK/STAT3

signaling pathway.

### Ethics approval and consent to participate

This study was approved by the Ethics Committee of the Third Affiliated Hospital of Sun Yat-Sen University (Approval No. [2016]2-26). All enrolled subjects provided written informed consent.

### Acknowledgements

We sincerely thank Xifu Wu for the human sample collection. We also would like to thank the biobank of clinical resources of the third affiliated hospital of Sun Yat-sen University for human samples conservation.

### Authorship contribution

HW established the mouse model, conducted IHC, IF, western

blot, TEER, hNECs culture and wrote the manuscript; YL performed qRT-PCR and cultured hNECs; XL participated in sample collection, hNECs culture and manuscript revision. WH and ZH participated in the sample collection. JM and UJ assisted in completing the experiment. YZ helped to design the study. GZ and LC designed the study and revised the manuscript.

### Conflict of interest

The authors claim that there are no conflicts of interest.

### Funding

This study was supported by the National Natural Science Foundation of China (82271145, 81970859, 82071020, and 82101196), the Natural Science Foundation of Guangdong Province (2023A1515012430), and the Science and Technology Planning Project of Guangzhou (2023A03J0208).

### References

- Bachert C, Marple B, Schlosser RJ, et al. Adult chronic rhinosinusitis. *Nat Rev Dis Primers* 2020; 6: 86.
- Sedaghat AR, Kuan EC, Scadding GK. Epidemiology of chronic rhinosinusitis: prevalence and risk factors. *J Allergy Clin Immunol Pract* 2022; 10: 1395-1403.
- Chee J, Pang KW, Low T, Wang Y, Subramaniam S. Epidemiology and aetiology of chronic rhinosinusitis in Asia-A narrative review. *Clin Otolaryngol* 2023; 48: 305-312.
- Fokkens WJ, Lund VJ, Hopkins C, et al. European Position Paper on Rhinosinusitis and Nasal Polyps 2020. *Rhinology* 2020; 58: 1-464.
- Sugita K, Steer CA, Martinez-Gonzalez I, et al. Type 2 innate lymphoid cells disrupt bronchial epithelial barrier integrity by targeting tight junctions through IL-13 in asthmatic patients. *J Allergy Clin Immunol* 2018; 141: 300-310.e11.
- Park SJ, Kim TH, Jun YJ, et al. Chronic rhinosinusitis with polyps and without polyps is associated with increased expression of suppressors of cytokine signaling 1 and 3. *J Allergy Clin Immunol* 2013; 131: 772-780.
- Tanaka S, Hirota T, Kamijo A, et al. Lung functions of Japanese patients with chronic rhinosinusitis who underwent endoscopic sinus surgery. *Allergol Int* 2014; 63: 27-35.
- Steelant B, Seys SF, Boeckstaens G, Akdis CA, Ceuppens JL, Hellings PW. Restoring airway epithelial barrier dysfunction: a new therapeutic challenge in allergic airway disease. *Rhinology* 2016; 54: 195-205.
- Singh N, Diebold Y, Sahu SK, Leonardi A. Epithelial barrier dysfunction in ocular allergy. *Allergy* 2022; 77: 1360-1372.
- Kirschner N, Rosenthal R, Furuse M, Moll I, Fromm M, Brandner JM. Contribution of tight junction proteins to ion, macromolecule, and water barrier in keratinocytes. *J Invest Dermatol* 2013; 133: 1161-1169.
- Rogers GA, Den Beste K, Parkos CA, Nusrat A, Delgado JM, Wise SK. Epithelial tight junction alterations in nasal polyposis. *Int Forum Allergy Rhinol* 2011; 1: 50-54.
- Meng J, Zhou P, Liu Y, et al. The development of nasal polyp disease involves early nasal mucosal inflammation and remodeling. *PLoS One* 2013; 8: e82373.
- Soyka MB, Wawrzyniak P, Eiwegger T, et al. Defective epithelial barrier in chronic rhinosinusitis: the regulation of tight junctions by IFN- $\gamma$  and IL-4. *J Allergy Clin Immunol* 2012; 130: 1087-1096.e10.
- Celebi Sozener Z, Ozdel Ozturk B, Cerci P, et al. Epithelial barrier hypohes: Effect of the external exposome on the microbiome and epithelial barriers in allergic disease. *Allergy* 2022; 77: 1418-1449.
- Li Y, Chang LH, Huang WQ, et al. IL-17A mediates pyroptosis via the ERK pathway and contributes to steroid resistance in CRSwNP. *J Allergy Clin Immunol* 2022; 150: 337-351.
- Pope JL, Ahmad R, Bhat AA, Washington MK, Singh AB, Dhawan P. Claudin-1 overexpression in intestinal epithelial cells enhances susceptibility to adenomatous polyposis coli-mediated colon tumorigenesis. *Mol Cancer* 2014; 13: 167.
- Song Y, Li Y, Xiao Y, et al. Neutralization of interleukin-17A alleviates burn-induced intestinal barrier disruption via reducing pro-inflammatory cytokines in a mouse model. *Burns Trauma* 2019; 7: 37.
- Wang X, Zhang N, Bo M, et al. Diversity of T(H) cytokine profiles in patients with chronic rhinosinusitis: A multicenter study in Europe, Asia, and Oceania. *J Allergy Clin Immunol* 2016; 138: 1344-1353.
- Chen X, Chang L, Li X, Huang J, Yang L, Lai X, et al. Tc17/IL-17A up-regulated the expression of MMP-9 via NF- $\kappa$ B pathway in nasal epithelial cells of patients with chronic rhinosinusitis. *Front Immunol* 2018; 9: 2121.
- Wu H, Wang Z, Li X, et al. IL-17A facilitates type 2 inflammation in a modified eosinophilic chronic rhinosinusitis mouse model. *Int Forum Allergy Rhinol* 2023; 13(9):1726-1737.
- Carlier FM, de Fays C, Pilette C. Epithelial Barrier Dysfunction in Chronic Respiratory Diseases. *Front Physiol* 2021; 12: 691227.
- Akdis CA. Does the epithelial barrier hypothesis explain the increase in allergy, autoimmunity and other chronic conditions. *Nat Rev Immunol* 2021; 21: 739-751.
- Markov AG, Aschenbach JR, Amasheh S. Claudin clusters as determinants of epithelial barrier function. *IUBMB Life* 2015; 67: 29-35.
- Kato A, Peters AT, Stevens WW, Schleimer RP, Tan BK, Kern RC. Endotypes of chronic rhinosinusitis: Relationships to disease phenotypes, pathogenesis, clinical findings, and treatment approaches. *Allergy* 2022; 77: 812-826.
- Bailey LN, Garcia J, Grayson JW. Chronic rhinosinusitis: phenotypes and endotypes. *Curr Opin Allergy Clin Immunol* 2021; 21: 24-29.
- Rha MS, Yoon YH, Koh JY, et al. IL-17A-producing sinonasal MALT cells in patients with chronic rhinosinusitis with nasal polyps. *J Allergy Clin Immunol* 2022; 149: 599-609.e7.
- Kleuskens M, Haasnoot ML, Herpers BM, et al. Butyrate and propionate restore interleukin 13-compromised esophageal epithelial barrier function. *Allergy* 2022; 77: 1510-1521.
- Ruiz García S, Deprez M, Lebrigand K, et al. Novel dynamics of human mucociliary differentiation revealed by single-cell RNA sequencing of nasal epithelial cultures. *Development* 2019; 146(20):dev177428..
- Davis AS, Chertow DS, Moyer JE, et al. Validation of normal human bronchial epi-

- thelial cells as a model for influenza A infections in human distal trachea. *J Histochem Cytochem* 2015; 63: 312-328.
30. Li J, Zhang L, Wu T, Li Y, Zhou X, Ruan Z. Indole-3-propionic acid improved the intestinal barrier by enhancing epithelial barrier and mucus barrier. *J Agric Food Chem* 2021; 69: 1487-1495.
  31. Li YH, Xiao HT, Hu DD, et al. Berberine ameliorates chronic relapsing dextran sulfate sodium-induced colitis in C57BL/6 mice by suppressing Th17 responses. *Pharmacol Res* 2016; 110: 227-239.
  32. Ramezani M, Moraitis S, Smith JL, Wormald PJ, Vreugde S. Th17 cytokines disrupt the airway mucosal barrier in chronic rhinosinusitis. *Mediators Inflamm* 2016; 2016: 9798206.
  33. Chen HL, Lo CH, Huang CC, Lu MP, Hu PY, Chen CS, et al. Galectin-7 downregulation in lesional keratinocytes contributes to enhanced IL-17A signaling and skin pathology in psoriasis. *J Clin Invest* 2021; 131(1):e130740.
  34. Qu M, Qi X, Wang Q, et al. Therapeutic Effects of STAT3 Inhibition on Experimental Murine Dry Eye. *Invest Ophthalmol Vis Sci* 2019; 60: 3776-3785.
  35. Tokunaga T, Sakashita M, Haruna T, et al. Novel scoring system and algorithm for classifying chronic rhinosinusitis: the JESREC Study. *Allergy* 2015; 70: 995-1003.
  36. Jin P, Zi X, Charn TC, et al. Histopathological features of antrochoanal polyps in Chinese patients. *Rhinology* 2018; 56: 378-385.
  37. Zhou AY, Taylor BE, Barber KG, et al. Anti-IL17A halts the onset of diabetic retinopathy in Type I and II diabetic mice. *Int J Mol Sci* 2023; 24(2):1347.
  38. Zhong Z, Su G, Kijlstra A, Yang P. Activation of the interleukin-23/interleukin-17 signaling pathway in autoimmune and autoimmune uveitis. *Prog Retin Eye Res* 2021; 80: 100866.
  39. Velasco E, Delicado-Miralles M, Hellings PW, Gallar J, Van Gerven L, Talavera K. Epithelial and sensory mechanisms of nasal hyperre-activity. *Allergy* 2022; 77: 1450-1463.
  40. Jiao J, Wang C, Zhang L. Epithelial physical barrier defects in chronic rhinosinusitis. *Expert Rev Clin Immunol* 2019; 15: 679-688.
  41. Schreiber S, Colombel JF, Feagan BG, et al. Incidence rates of inflammatory bowel disease in patients with psoriasis, psoriatic arthritis and ankylosing spondylitis treated with secukinumab: a retrospective analysis of pooled data from 21 clinical trials. *Ann Rheum Dis* 2019; 78: 473-479.
  42. Eshwar V, Kamath A, Shastry R, Shenoy AK, Kamath P. A review of the safety of Interleukin-17A inhibitor secukinumab. *Pharmaceuticals (Basel)* 2022; 15: 1365.
  43. van de Kerkhof PC, Griffiths CE, Reich K, Leonardi CL, Blauvelt A, Tsai TF, et al. Secukinumab long-term safety experience: A pooled analysis of 10 phase II and III clinical studies in patients with moderate to severe plaque psoriasis. *J Am Acad Dermatol* 2016; 75: 83-98.e4.
  44. Wise SK, Laury AM, Katz EH, Den Beste KA, Parkos CA, Nusrat A. Interleukin-4 and interleukin-13 compromise the sinonasal epithelial barrier and perturb intercellular junction protein expression. *Int Forum Allergy Rhinol* 2014; 4: 361-370.
  45. Mahdavinia M, Bishehsari F, Hayat W, et al. Prevalence of allergic rhinitis and asthma in patients with chronic rhinosinusitis and gastroesophageal reflux disease. *Ann Allergy Asthma Immunol* 2016; 117: 158-162.e1.
  46. Ramakrishnan VR, Gonzalez JR, Cooper SE, et al. RNA sequencing and pathway analysis identify tumor necrosis factor alpha driven small proline-rich protein dysregulation in chronic rhinosinusitis. *Am J Rhinol Allergy* 2017; 31: 283-288.
  47. Heijink IH, Brandenburg SM, Postma DS, van Oosterhout AJ. Cigarette smoke impairs airway epithelial barrier function and cell-cell contact recovery. *Eur Respir J* 2012; 39: 419-428.
  48. Zhang Z, Li G, Yu L, et al. Causal relationships between potential risk factors and chronic rhinosinusitis: a bidirectional two-sample Mendelian randomization study. *Eur Arch Otorhinolaryngol* 2023; 280: 2785-2793.

Gehua Zhang, M.D., Ph.D.  
 Department of Otolaryngology  
 Head and Neck Surgery  
 The Third Affiliated Hospital of Sun  
 Yat-Sen University  
 No. 600 Tianhe Road  
 Guangdong  
 Guangzhou 510630  
 China

Tel: +86-20-85253045  
 E-mail: zhanggeh@mail.sysu.edu.cn

Lihong Chang, M.D., Ph.D.  
 Department of Otolaryngology  
 Head and Neck Surgery  
 The Third Affiliated Hospital of Sun  
 Yat-Sen University  
 No. 600 Tianhe Road  
 Guangdong  
 Guangzhou 510630  
 China

Tel: +86-20-85253045  
 E-mail: changlh3@mail.sysu.edu.cn

Haotian Wu<sup>#</sup>, Yue Li<sup>#</sup>, Xia Li<sup>#</sup>, Weiqiang Huang, Zizhen Huang, Xiaoping Lai,  
 Junming Ma, Yanjie Jiang, Yana Zhang, Lihong Chang\*, Gehua Zhang\*

Department of Otorhinolaryngology-Head and Neck Surgery, the Third Affiliated Hospital of Sun Yat-Sen University,  
 Guangzhou, China

<sup>#</sup> These authors contributed equally to the completion of this article

\* These authors contributed equally to design and supervise this study

**Rhinology** 62: 6, 726 - 738, 2024  
<https://doi.org/10.4193/Rhin24.127>

**Received for publication:**

March 23, 2024

**Accepted:** September 7, 2024

**Associate Editor:**

Ahmad Sedaghat

**This manuscript contains online supplementary material**

## SUPPLEMENTARY MATERIAL

### Subjects and evaluation

This study was approved by the Ethics Committee of the Third Affiliated Hospital of Sun Yat-sen University (approval no. [2016]2-26). Nasal tissue samples were collected from inpatients, including 34 patients with CRSsNP, 36 patients with CRSwNP, and 39 control subjects who underwent nasal endoscopic surgery at the Third Affiliated Hospital of Sun Yat-Sen University. CRSsNPs and CRSwNPs were diagnosed and classified according to EPOS 2020 guidelines. The nasal mucosa and polyps samples were collected from the osteomeatal complexes of patients with CRSsNP and CRSwNP, respectively. Nasal mucosa of the inferior turbinate was collected from control subjects with nasal septal deviations. All patients with CRS discontinued oral corticosteroids and antibiotics for at least three months and topical corticosteroids for at least one month before surgery. The atopic status of the subjects was evaluated using EUROLINE Atopy (China) (IgE) detection and total IgE detection kits (EUROIMMUN, PerkinElmer). Patients were diagnosed as atopic if their allergen-specific IgE level was > 3.51 kU/L. Asthma was diagnosed by an allergist based on medical history and lung function analysis. Patients with autoimmune diseases, severe systemic diseases, primary ciliary dyskinesia, cystic fibrosis, acute infections, fungal sinusitis, systemic vasculitis, or non-steroidal anti-inflammatory drug-exacerbated respiratory disease (N-ERD) were excluded. The samples were subdivided into three pieces: one was stored at -80°C for subsequent RT-qPCR analysis; another was fixed in 4% paraformaldehyde for paraffin embedding for further immunohistochemistry and immunofluorescence staining; and the remaining tissue was placed in PBS at 4°C for subsequent primary human nasal epithelial cell (hNECs) culture. Due to the limited amount of tissue available for biopsy, not all samples were included in each study method. The clinical data of the patients used in the experiments are summarized in Tables S1 and S2.

### Immunohistochemistry and immunofluorescence

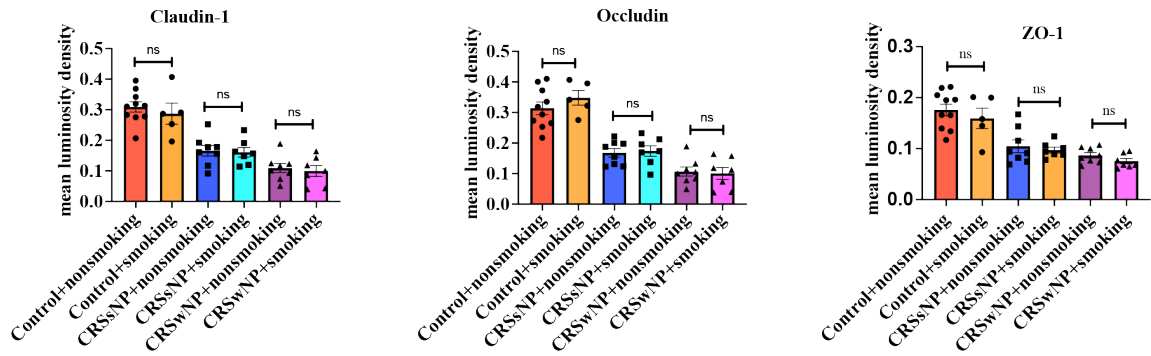
Paraffin sections of human and mouse nasal mucosal tissues were deparaffinized and rehydrated at room temperature. The sections were then permeabilized with 2% Triton X-100 (So-

larbio, Beijing, China) at room temperature for 10 minutes and blocked with 10% goat serum (Bioss Antibodies, Beijing, China) for 60 minutes. The sections were then incubated overnight at 4°C with anti-IL-17A, anti-claudin-1, anti-occludin, anti-ZO-1 (Proteintech, Chicago, USA). For immunohistochemistry, the sections were incubated with horseradish peroxidase-conjugated goat anti-rabbit secondary antibody (Immunoway, Jiangsu, China) at room temperature for 1 hour. This was followed by incubation with diaminobenzidine (DAB; Zhongshan Golden Bridge, Beijing, China) and counterstaining with hematoxylin. The sections were observed under an optical microscope. For immunofluorescence detection, sections were incubated with Alexa Fluor 488-conjugated goat anti-rabbit secondary antibody or Alexa Fluor 594-conjugated goat anti-rabbit secondary antibody (both from Invitrogen, Carlsbad, CA, USA) at room temperature for 1 hour, followed by DAPI nuclear staining. Images were captured using an upright fluorescence microscope. Immunofluorescence staining of air-liquid interface (ALI)-cultured hNECs followed the same procedure. The samples were then incubated with anti-claudin-1, anti-occludin, anti-ZO-1 (Proteintech, Chicago, USA), anti-p-ERK, anti-p-STAT3, anti-ERK, anti-STAT3 antibody (all from Affinity, Jiangsu, China) and images were captured using a confocal laser scanning fluorescence microscope. ImageJ software was utilized for the quantitative analysis of p-ERK, p-STAT3, ERK, STAT3, claudin-1, occludin, and ZO-1 expression in random high-power fields. anti-p-ERK, anti-p-STAT3, anti-ERK, anti-STAT3 antibody (all from Affinity, Jiangsu, China).

### Air-liquid interface (ALI) culture and treatment of hNECs

The air-liquid interface (ALI)-cultured hNECs were cultured according to the procedures described in the Methods section of the manuscript. After 14 days of culture, the culture medium in the lower chamber was replaced with ALI culture medium containing 300 ng/mL of recombinant human IFN- $\gamma$ , recombinant human IL-4, and recombinant human IL-13 were added to the corresponding lower chamber. The cells were then cultured for an additional 24 hours. For the control group, the medium was replaced with a freshly prepared ALI culture medium.

**A**



**B**

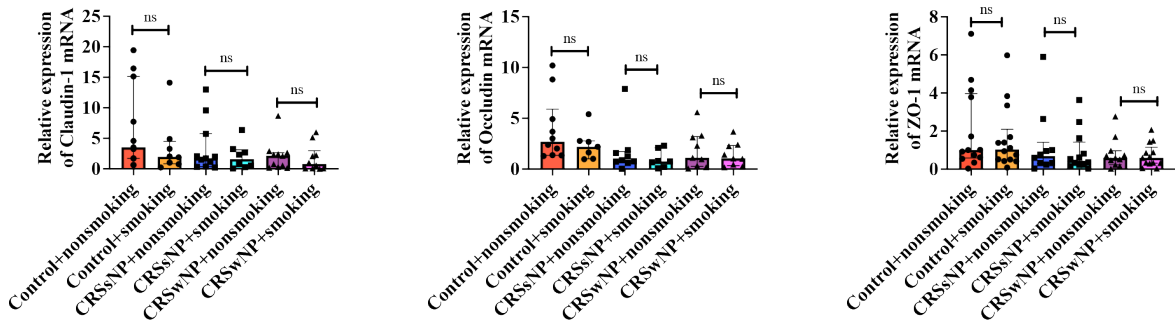


Figure S1. Expressions of tight junction proteins in the nasal mucosal tissues of smoking and non-smoking patients with chronic rhinosinusitis and healthy controls. A) Quantitative analysis of the immunohistochemical staining of tight junction proteins in the nasal mucosal tissues was conducted on samples from smoking and non-smoking patients with chronic rhinosinusitis and healthy controls. Data are presented as means  $\pm$  SEMs. B) Quantitative analysis of mRNA expressions of claudin-1, occludin, and ZO-1 in the nasal mucosal tissues of the controls and patients with CRSsNP and CRSwNP. Mann-Whitney test. FigE1A, smoking control subjects, n = 5; non-smoking control subjects, n = 10; smoking CRSsNP patients and smoking CRSwNP patients, both n = 7; non-smoking CRSsNP patients and non-smoking CRSwNP patients, both n = 8. FigE1B, smoking control subjects, n = 8-14; non-smoking control subjects, n = 10-13; smoking CRSsNP patients, n = 7-12; non-smoking CRSsNP patients, n = 9-11; smoking CRSwNP patients, n = 9-14; non-smoking CRSwNP patients, n = 9-11.

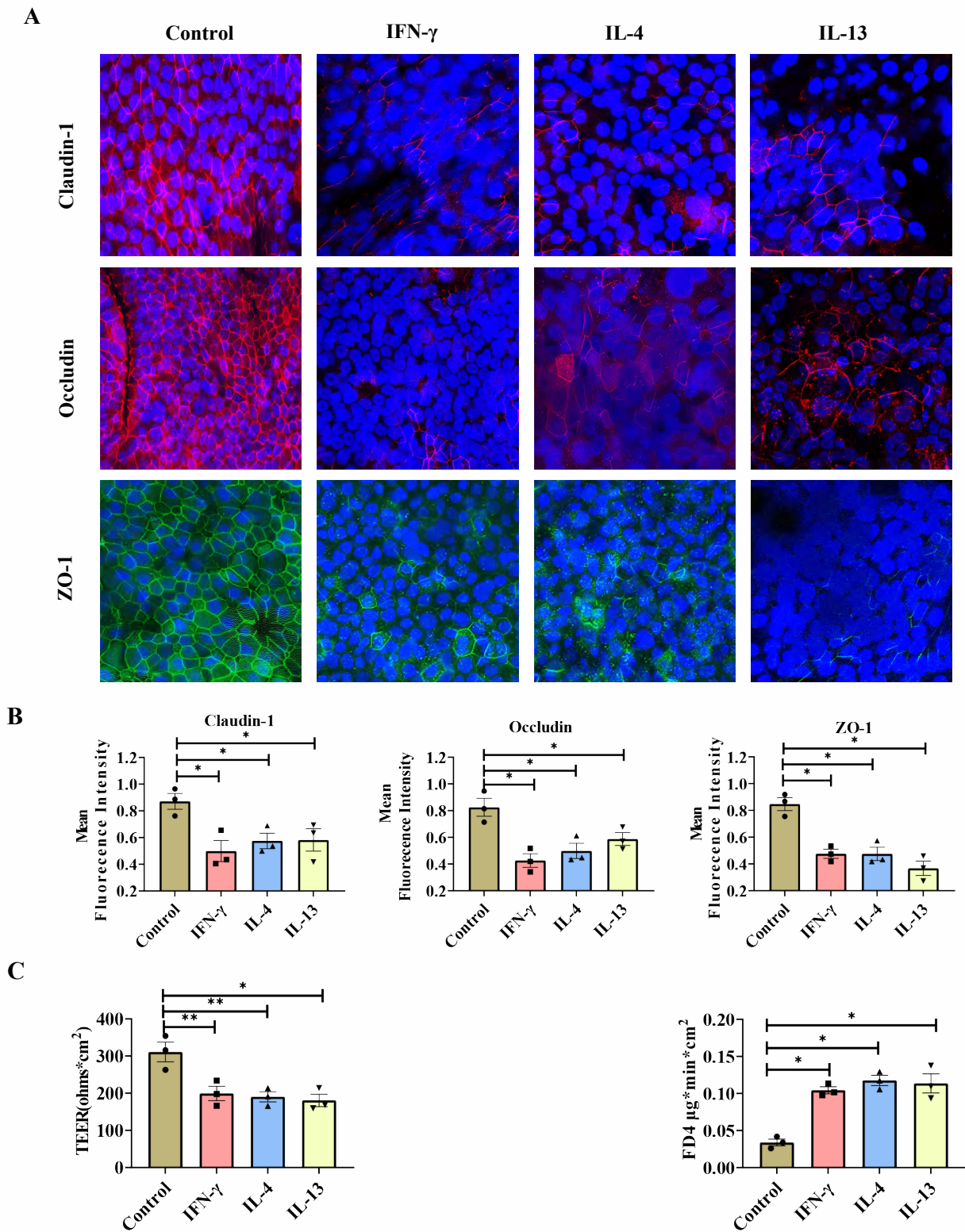


Figure S2. Type 2 inflammatory cytokines IL-4, IL-13, and type 1 inflammatory cytokine IFN- $\gamma$  disrupted the epithelial barrier in hNECs.

A) Immunofluorescence staining of tight junction proteins in hNECs cultured in ALI after different treatments (confocal microscopy 630 $\times$ ). B) Quantitative analysis of expressions of claudin-1, occludin, and ZO-1 in hNECs cultured in ALI with different treatments. C) TEER and FD4 permeability experiments to assess transmembrane resistance and permeability in hNECs cultured in ALI with different treatments. Data presented as means  $\pm$  SEMs. \* $p < 0.05$ , \*\* $p < 0.01$ . 3 biopsy specimens in each group.

Table S1. Demographic characteristics of enrolled subjects for detecting the expressions of TJ proteins

	Control	CRSsNP	CRSwNP
<b>Total subjects enrolled</b>	39	34	36
<b>Methodology used</b>			
<b>Histology study</b>			
N	15	15	15
Gender, male (%)	10 (66.6%)	11 (73.3%)	11 (73.3%)
Age, Mean (95%CI)	36 (23, 47)	41 (31, 53)	45 (33, 67)
Atopy, N (%)	3 (20%)	3 (20%)	5 (33.3%)
AR, N (%)	3 (20%)	3 (20%)	5 (33.3%)
Asthma, N (%)	0 (0%)	0 (0%)	0 (0%)
Smoking, N (%)	5 (33.3%)	7 (46.6%)	7 (46.6%)
<b>RT-PCR</b>			
N	27	22	25
Gender, male (%)	14 (51.8%)	15 (68.1%)	13 (52%)
Age, Mean (95%CI)	31 (12, 50)	35 (18, 50)	37 (18, 56)
Atopy, N (%)	1 (4%)	2 (9%)	3 (12%)
AR, N (%)	3 (11%)	2 (9%)	7 (28%)
Asthma, N (%)	0 (0%)	0 (0%)	0 (0%)
Smoking, N (%)	14 (51.8%)	12 (54.5%)	14 (56%)

Histology study included immunohistochemistry and immunofluorescence.

Table S2. Demographic characteristics of enrolled CRSwNP patients used for hNECs culture.

	Immunofluorescence	Western Blotting	TEER and FD4
N	10	5	10
Gender, male (%)	6 (60%)	3 (60%)	6 (60%)
Age, Mean (95%CI)	41 (29,51)	37 (29,46)	42 (31,51)
Atopy, N (%)	0 (0)	0 (0)	1 (16.6%)
AR, N (%)	0 (0)	0 (0)	1 (16.6%)
Asthma, N (%)	0 (0)	0 (0)	0 (0)

Table S3. Primers used for quantitative RT-PCR analysis

Primer	Sequence	Annealing temperature (°C)
Claudin-1	(F) 5'- CAACATACAGTGACGCTTCACA-3'	60
	(R) 5'- CACTATTGACGTTTCCCCACTC-3'	
Occludin	(F) 5'-ACAAGCGGTTTATCCAGAGTC-3'	60
	(R) 5'- GTCATCCACAGGCGAAGTTAAT-3'	
ZO-1	(F) 5'- CAACATACAGTGACGCTTCACA-3'	60
	(R) 5'- CACTATTGACGTTTCCCCACTC-3'	